

# Ti:sapphire-laser-based resonance-scattering lidar system for simultaneous observation of Ca and Ca<sup>+</sup> layers appearing in the upper atmosphere

Ayaka Hashimoto<sup>(a)</sup>, Mitsumu K. Ejiri<sup>(b,c)</sup>, Sota Kobayashi<sup>(a)</sup>, Sayako Miyoshi<sup>(a)</sup>, Megumi Ootose<sup>(a)</sup>, Chiaki Ohae<sup>(a,d)</sup>, Takuji Nakamura<sup>(b,c)</sup>, and Masayuki Katsuragawa<sup>(a,b,d,\*)</sup>

<sup>(a)</sup> Graduate School of Informatics and Engineering, University of Electro-Communications  
1-5-1 Chofugaoka, Chofu, Tokyo 182-8585, Japan

<sup>(b)</sup> National Institute of Polar Research,  
10-3 Midoricho, Tachikawa, Tokyo 190-8518, Japan

<sup>(c)</sup> The Graduate University for Advanced Studies, SOKENDAI  
10-3 Midoricho, Tachikawa, Tokyo 190-8518, Japan

<sup>(d)</sup> Institute for Advanced Science, University of Electro-Communications  
1-5-1 Chofugaoka, Chofu, Tokyo 182-8585, Japan

<sup>(\*)</sup>Lead Author e-mail address: [katsuragawa@uec.ac.jp](mailto:katsuragawa@uec.ac.jp)

**Abstract:** Meteoric atoms and ions are among the remarkable tracers to investigate a variety of dynamics appearing in the mesosphere and thermosphere at altitudes ranging from 80 to 150 km. Here, we report on a solid-laser-based lidar system, namely dual-wavelength injection-locked nanosecond-pulsed Ti:sapphire lidar, that can simultaneously detect resonance scatterings by meteoric calcium atom (Ca) and ion (Ca<sup>+</sup>) layers. We operated the lidar system and conducted a benchmark test in which Ca or Ca<sup>+</sup> was observed independently as a first step. We found that the lidar system was operated stably over an entire night, having the ability to detect either Ca or Ca<sup>+</sup> with a sufficient signal-to-noise ratio in addition to high temporal and spatial resolutions. In our presentation, we also report on a typical demonstration of the lidar system, namely the observation of Ca and Ca<sup>+</sup> over an entire night.

## 1. Introduction

Meteoric atoms and ions distributed in the mesosphere and lower thermosphere are among the remarkable tracers that can provide important knowledge on the dynamics of the whole atmosphere, in which the troposphere, stratosphere, mesosphere, and thermosphere are linked with each other. A variety of lidar observations targeting such meteoric atoms and ions have been examined so far [1]. Continuous lidar observations over a long time in which iron or sodium neutral atoms are employed as tracers are also being conducted in several observatories across the world [1]. Lasers are at the core of such lidar systems, and a variety of types, including dye lasers, alexandrite lasers, and YAG lasers, are utilized. In 2023, an OPO (optical parametric oscillator) solid-laser-based lidar system, in which calcium ion was targeted as a tracer, was also reported [2].

Here, we report a new solid-laser based-lidar system, namely the dual-wavelength injection-locked nanosecond-pulsed Ti:sapphire lidar. The remarkable feature of this lidar system is its ability to simultaneously emit dual-wavelength radiation, which is resonant to Ca and Ca<sup>+</sup> [3,4], from a single laser resonator. We operated the lidar system and conducted a benchmark test in which Ca or Ca<sup>+</sup> was observed separately as a first step. The lidar system was operated stably over an entire night and showed an ability to detect either Ca or Ca<sup>+</sup> with a sufficient signal-to-noise ratio in addition to high temporal and spatial resolutions.

## 2. Dual-wavelength injection-locked nanosecond pulsed Ti:sapphire laser for a calcium lidar system

Figure 1 illustrates the configuration of the developed laser system. The entire system consists of two ECLDs (external-cavity-

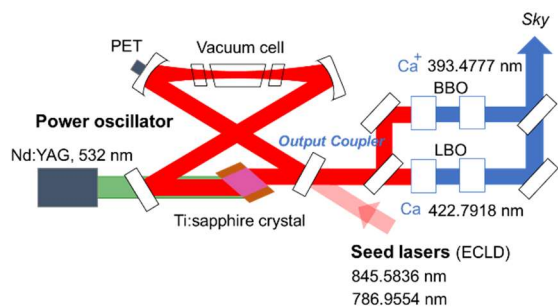


Figure 1. Configuration of dual-wavelength injection-locked nanosecond-pulsed Ti:sapphire laser for the calcium lidar system.

controlled laser diodes) as seed lasers and a ring Ti:sapphire laser as a power oscillator [5-9]. The oscillation wavelengths of the two seed lasers are respectively tuned to the resonant wavelengths of Ca (845.5836 nm: 422.7918 nm  $\times$  2) and Ca<sup>+</sup> (786.9554 nm: 393.4777 nm  $\times$  2). A notable feature of this laser system is that the output coupler of the ring resonator is designed to have the correct wavelength-dependent reflectivity, enabling simultaneous injection-locked pulsed oscillation at the two resonant wavelengths of Ca and Ca<sup>+</sup> despite a wide wavelength spacing exceeding 50 nm between the two resonant wavelengths.

The pulsed outputs were, in reality, injection locked by the two seed lasers, stably generating Fourier-transform-limited nanosecond pulses (35 MHz, 12 ns at 787 nm; 25 MHz, 13 ns at 846 nm), with carrier wavelengths identical to those of the two seed lasers. The two-wavelength nanosecond-laser pulses overlapped perfectly in time and space, as they were output from a single laser resonator [4]. The maximum pulsed energy was 20 mJ/pulse. The long-term operational output energy was, however, set to 10 mJ/pulse (the sum of the pulsed outputs at the two seed wavelengths) at a 100-Hz repetition rate. We took damage of the optical components into consideration.

### 3. Observation of meteoric calcium atoms and ions by using the developed Ti:sapphire-laser based lidar system

We operated the resonance scattering lidar system and conducted a benchmark test. The receiver was configured by using a Nasmyth-type telescope with a 80-cm aperture and a photon-counting-type data-accumulation system (Licel).

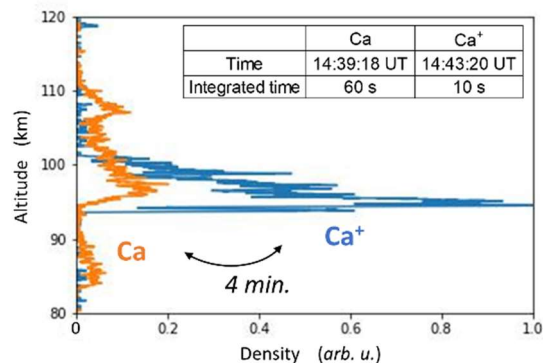


Figure 2. Density distributions of Ca and Ca<sup>+</sup> as functions of altitude, as observed by using the Ti:sapphire-laser-based lidar system.

As a first step, on 27 July 2022 we performed observations independently targeting Ca and Ca<sup>+</sup>. The averaged laser powers were controlled at 0.5 W for Ca and 0.4 W for Ca<sup>+</sup>. The temporal and spatial resolutions were set at 60 s and 15 m, respectively, for Ca and 10 s and 15 m for Ca<sup>+</sup>. Figure 2 shows typical resonance scattering signals from the Ca (orange) and Ca<sup>+</sup> (blue) layers, detected as a function of altitude. The resonance scattering signals from the high-altitude region of 80 to 120 km were measured with a sufficient signal-to-noise ratio in addition to high temporal and spatial resolutions. The time difference between the Ca and Ca<sup>+</sup> observations was about 4 min, suggesting that the Ca and Ca<sup>+</sup> were, in reality, simultaneously distributed, as seen in Figure 2.

As a next step, we conducted continuous observations of Ca and Ca<sup>+</sup> over an entire night. The relevant conditions for the observations,

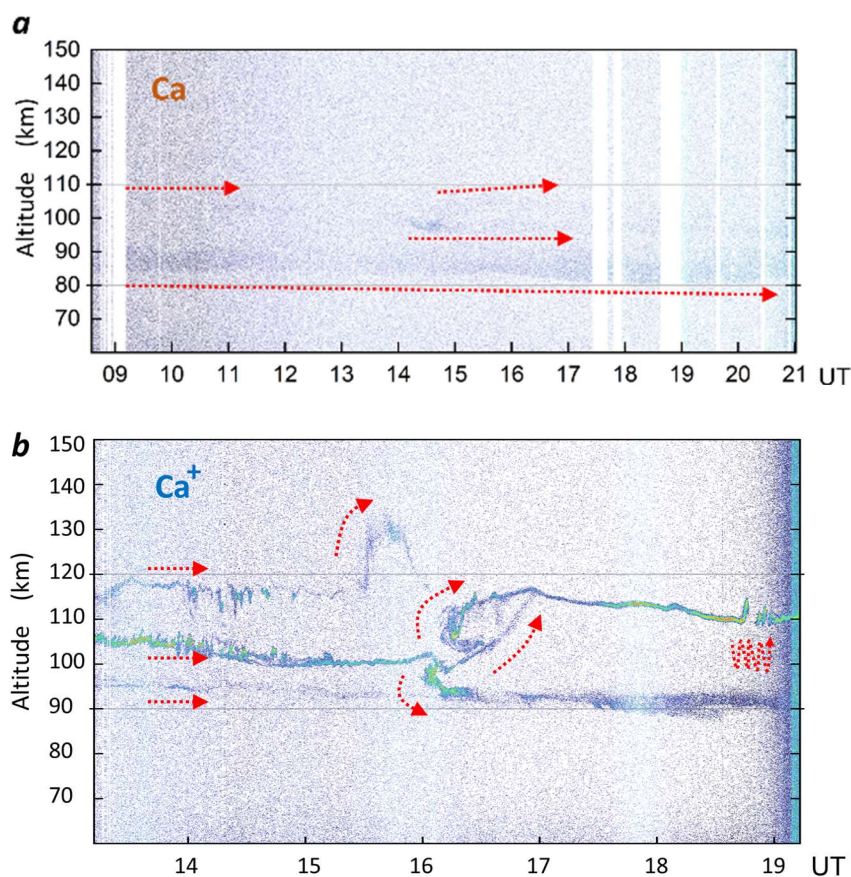


Figure 3. Observations taken over entire nights. *a*, Ca layer (19 December 2022) and *b*, Ca<sup>+</sup> layer (9 August 2022)

such as output power, and the temporal and spatial resolutions, were determined on the basis of the results of the preliminary test in Figure 2. They were, respectively, 0.5 W, 30 s, and 15 m for Ca (operated on 19 December 2022 over 12 h) and 0.4 W, 30 s, and 15 m for Ca<sup>+</sup> (operated on 9 August 2022 over 6 h). As is apparent in Figures 3a and 3b, we were able to observe in detail the behaviors of the Ca and Ca<sup>+</sup> layers continuously over an entire night. The multiple layers of both Ca or Ca<sup>+</sup> varied dynamically in a complex way. The Ti:sapphire-laser-based lidar system featured these detailed structures with high temporal and spatial resolutions.

In our presentation, we will also report on our progress with respect to the simultaneous

observation of Ca and Ca<sup>+</sup> dynamics, which is currently ongoing.

[1] X. Chu and G. C. Papen, Resonance fluorescence lidar for measurements of the middle and upper atmosphere, In T. Fujii and T. Fukuchi (Eds.), *The Book of Laser Remote Sensing* (pp. 179–432). Boca Raton, Fla: CRC Press, Taylor and Francis Group.  
 [2] J. Jiao, X. Chu, H. Jin, Z. Wang, Y. Xun, L. Du, et al., “First lidar profiling of meteoric Ca<sup>+</sup> ion transport from ~80 to 300 km in the midlatitude nighttime ionosphere,” *Geophysical Research Letters* **49**, e2022GL100537 (2022).  
 [3] M. Gerding, M. Alpers, and U. von Zahn, “Atmospheric Ca and Ca<sup>+</sup> layers: Midlatitude observations and Modeling,” *J. Geophys. Res.* **105**, 27,131-27,146 (2000).

- [4] Mitsumu K. Ejiri, Takuji Nakamura, Takuo T. Tsuda, Takanori Nishiyama, Makoto Abo, Chiao-Yao She, Michi Nishioka, Akinori Saito, Toru Takahashi, Katsuhiko Tsuno, Takuya D. Kawahara, Takayo Ogawa, Satoshi Wada, “Observation of synchronization between instabilities of the sporadic E layer and geomagnetic field line connected F region medium-scale traveling ionospheric disturbances,” *J. Geophys. Res: Space Physics* **124**, 4627-4638 (2019).
- [5] M. Katsuragawa and T. Onose, “Dual-Wavelength Injection-Locked, Pulsed Laser,” *Optics Letters* **30**, 2421-2423 (2005).
- [6] T. Onose and M. Katsuragawa, “Dual-wavelength injection-locked, pulsed laser with precisely predictable performance,” *Optics Express*. **15**, 1600-1605 (2007).
- [7] Y. Fujii and M. Katsuragawa, “Dual frequency pulsed laser with an accurate gigahertz-beat-note,” *Optics Letters*, **15**, 3065-3067 (2007).
- [8] T. Gavara, T. Ohashi, Y. Sasaki, T. Kawashima, H. Hamano, R. Yoshizaki, Y. Fujimura, K. Yoshii, C. Ohae, and M. Katsuragawa, “Dual-frequency injection-locked continuous-wave near-infrared laser,” *Optics Letters*. **41**, 2994 – 2997 (2016).
- [9] M. Katsuragawa, C Ohae, US10,763,634B2 (2016/11/16).